Meiotic interactors of a mitotic gene *TAO3* revealed by functional analysis of its rare variant

Saumya Gupta[*], Aparna Radhakrishnan[*], Rachana Nitin[*], Pandu Raharja-Liu[†], Gen Lin[‡], Lars M. Steinmetz[‡,§,**], Julien Gagneur[†,††], Himanshu Sinha[*,1]

[*]Department of Biological Sciences, Tata Institute of Fundamental Research, Mumbai 400005, India

[†]Gene Center, Ludwig-Maximilians-Universität, 81377 Munich, Germany

[‡]European Molecular Biology Laboratory, Genome Biology Unit, 69117 Heidelberg, Germany

[§]Department of Genetics, Stanford University School of Medicine, Stanford, California 94305

[**]Stanford Genome Technology Center, Stanford University, Palo Alto, California 94304

[††]Technische Universität München, Department of Informatics, 85748 Garching, Germany

[1]**Corresponding author:** Department of Biological Sciences, Tata Institute of Fundamental Research, Homi Bhabha Road, Colaba, Mumbai 400005, India. Email: hsinha@tifr.res.in

Running title:

Role of mitotic gene *TAO3* in meiosis

Keywords:

Rare variant, *TAO3*, meiosis, transcriptome profiling, allelic variant

ABSTRACT

Studying the molecular consequences of rare genetic variants has the potential of identifying novel and hereto uncharacterized pathways causally contributing to phenotypic variation. Here we characterize the functional consequences of a rare coding variant of *TAO3*, previously reported to significantly contribute to sporulation efficiency variation in *Saccharomyces cerevisiae*. During mitosis *TAO3* interacts with *CBK1*, a conserved NDR kinase and a component of RAM network. The RAM network genes are involved in regulation cell separation and polarization. We demonstrate that the role of the rare allele *TAO3(4477C)* in meiosis is distinct from its role in mitosis by being independent of *ACE2*, which is a RAM network target gene. By quantitatively measuring cell morphological dynamics and conditionally expressing *TAO3(4477C)* allele during sporulation, we show that *TAO3* has an early role in meiosis. This early role of *TAO3* coincides with entry of cells into meiotic division. Time-resolved transcriptome analyses during early sporulation phase identified regulators of carbon and lipid metabolic pathways as candidate mediators. We experimentally show that during sporulation the *TAO3* allele genetically interacts with *ERT1* and *PIP2*, the regulators of tricarboxylic acid cycle and gluconeogenic enzymes, respectively. We thus uncover meiotic functions of *TAO3*, a mitotic gene and propose *ERT1* and *PIP2* as novel regulators of sporulation efficiency. Our results demonstrate that study of causal effects of genetic variation on the underlying molecular network has the potential to provide more extensive comprehension of the pathways driving a complex trait. This can help identify prospective personalized targets for intervention in complex diseases.

INTRODUCTION

The 'common disease, common variant' rationale of genome-wide association studies is being challenged owing to limited fraction of disease heritability explained by the mapped common variants (Manolio *et al.* 2009; Zuk *et al.* 2014). One of the potential contributors to this 'missing' heritability has been suggested to be the potential effects of rare variants which are not considered (Saint Pierre and Génin 2014). This view has been substantiated by the identification of rare variants carrying a considerable risk for autism, schizophrenia and epilepsy (Stankiewicz and Lupski 2010). Thus characterizing the functional role of rare variants associated with complex diseases has the potential for revealing new biology and providing opportunities for treatment (Cirulli and Goldstein 2010; Zuk *et al.* 2014). Even though multiple variants for various diseases have been mapped, they have not been able to provide targets for treatment. This is because firstly, many variants have been mapped in regulatory or non-coding regions, therefore the affected gene is not known. Secondly, even when a variant is in a coding sequence but if the affected gene is not well characterized for the phenotype, the variant may be of little use. This makes characterization of either common or rare genetic variants laborious. Hence the causal path connecting a variant to the phenotype is usually unknown. Thus to understand the causal path of a variant, it is important to identify the mediating molecular pathways. Identifying these mediating pathways has the potential to greatly expand the set of possible targets for molecular intervention (Gagneur *et al.* 2013).

Yeast sporulation efficiency is a complex trait and many causative polymorphisms have been mapped in sporulation genes such as *IME1*, an initiator of meiosis (Gerke *et al.* 2009) and *RIM15*, a glucose-sensing regulator of meiosis (Lorenz and Cohen 2014). However a polymorphism each was identified in two genes with functional annotations described for mitotic growth only. These polymorphisms were in *MKT1*, a putative RNA-binding protein and *TAO3*, a putative scaffolding protein (Deutschbauer and Davis 2005). These novel non-synonymous polymorphisms, *MKT1(89G)* and *TAO3(4477C)* were identified in a high efficiency sporulating SK1 strain while the low efficiency S288c strain had *MKT1(89A)* and *TAO3(4477G)* (Deutschbauer and Davis 2005). In our previous work we determined that *MKT1(89G)* variant increased the sporulation efficiency by genetically interacting with regulators of mitochondrial retrograde signaling and nitrogen starvation during sporulation (Gupta *et al*. 2015). Tao3 encodes a highly conserved scaffolding protein that is a component

84 of the RAM (Regulation of Ace2p activity and cellular Morphogenesis) signaling network.
85 Tao3 is required for activation and localization of an NDR protein kinase Cbk1, another
86 essential component of RAM network (Du and Novick 2002; Hergovich *et al.* 2006). This
87 RAM signaling network including Cbk1, Hym1, Kic1, Mob2 and Tao3 contributes to various
88 important processes of mitotic cellular growth. Regulation of transcription factor Ace2 by the
89 RAM network is critical for cell separation and polarized growth (Nelson *et al*. 2003). Ace2
90 peaks early in mitosis and is involved in G_1/S transition (Spellman *et al.* 1998). This RAM
91 network also known to regulate cellular progression through a Ace2-independent pathway
92 (Bogomolnaya *et al.* 2006). However none of these *TAO3* mitotic interactions provide clues
93 for its role in the developmental process of meiosis and sporulation.
94
95 Here we characterized the functional role of *TAO3(4477C)* in sporulation efficiency variation
96 by elucidating the molecular pathways linking this mitotic gene in meiosis. We compared
97 phenotypes of a pair of S288c-background strains differing only for the casual *TAO3*
98 polymorphism. Genome-wide transcriptional dynamics during sporulation of these strains
99 identified candidate mediator genes. Allele-specific genetic interaction assay between these
100 candidate genes and casual *TAO3* allele identified the regulators of tricarboxylic acid cycle
101 and gluconeogenic enzymes as casual and novel regulators of sporulation efficiency.
102

103 # RESULTS

104 **Role of causative allele of *TAO3* in sporulation efficiency variation**

105 Analysis of *TAO3* sequence of 38 *S. cerevisiae* strains in the Saccharomyces Genome
106 Resequencing Project (SGRP) database (Liti *et al.* 2009) and 24 strains in Saccharomyces
107 Genome Database (SGD), showed that *TAO3(4477C)* allele of SK1 strain was a rare variant
108 (minor allele frequency = 1.6%, Figure 1A). Deutschbauer and Davis (2005) mapped this rare
109 variant as a causal allele for increased sporulation efficiency in a cross between S288c (low
110 sporulating) and SK1 (high sporulating) strains and introduced it in the S288c background to
111 construct allele replacement strain YAD331. This allele replacement strain differed from the
112 parental S288c strain (*TAO3(4477G)*) only for this variant. A clean allele replacement strain,
113 termed as "T strain" was constructed from YAD331 (see Methods) and its sporulation
114 efficiency at 48h was reconfirmed to be three-fold higher than the S288c strain (termed as "S
115 strain", $P = 1.8 \times 10^{-10}$, pair test in Methods, Figure 1B). This fold-difference remained
116 constant even after a week of incubation (Figure 1C). Studying the progression of meiotic

117 phases showed that the T strain initiated meiosis within 12h (Figure 1D-E). Quantitative
118 comparison of the time to initiate meiosis and the rate of transition from G_1/G_0 into Meiosis I
119 stage showed significant difference between the T and S strains (Figure 1D-E, Figure S1).
120 This suggested that *TAO3(4477C)* affected entry of the T strain cells initiating meiosis within
121 12h in sporulation. To resolve when during this 12h time phase *TAO3(4477C)* affects the
122 phenotype, this endogenous allele in the T strain was placed under a tetracycline-responsive
123 promoter (P_{Tet}-*TAO3(4477C)* strain, see Methods). In the absence of tetracycline analogue,
124 doxycycline, P_{Tet}-*TAO3(4477C)* strain showed higher expression of *TAO3(4477C)* relative to
125 its expression in the S strain (Methods, Figure S2). Addition of 2µg/ml doxycycline
126 significantly reduced *TAO3* expression level, making it equivalent to the S strain (Methods,
127 Figure S2). Concomitantly in the absence of doxycycline, the P_{Tet}-*TAO3(4477C)* strain
128 showed high sporulation efficiency (Figure 1F). In presence of doxycycline for the entire 48h
129 in sporulation medium, the sporulation efficiency of the P_{Tet}-*TAO3(4477C)* strain was
130 equivalent to the S strain (Figure 1F). This suggested that high *TAO3(4477C)* expression was
131 required for the high sporulation efficiency phenotype. We next reduced *TAO3(4477C)*
132 expression for specific shorter time-periods in the sporulation medium. Sporulation efficiency
133 of the P_{Tet}-*TAO3(4477C)* strain was equivalent whether doxycycline was present only for the
134 first 6h or for 48h and this efficiency was equivalent to the S strain (Figure 1F). However
135 when doxycycline was present only for the first 3h, the P_{Tet}-*TAO3(4477C)* strain showed a
136 slight but significant difference (P = 0.02) in sporulation efficiency compared to S strain
137 (Figure 1F). This showed that *TAO3(4477C)* allele affected sporulation efficiency within the
138 first 6h in sporulation.
139
140 **Role of *TAO3* in meiosis is distinct from its role during mitosis**
141 Varying the gene expression of *TAO3(4477C)* affected the sporulation efficiency phenotype.
142 Hence to identify the molecular pathways affected by this causative allele, we studied the
143 global gene expression dynamics during sporulation in the allele replacement strains. Time-
144 resolved transcriptomics of the T and S strains were compared from 0h to 8h30m in
145 sporulation medium (see Methods). At the initial time point (t = 0h) only 190 out of 6,960
146 transcripts (~3%) showed differential expression, with an enrichment for a single gene
147 ontology term iron ion homeostasis (P = 0.04, post Holm-Bonferroni corrected, Figure S3).
148 In contrast 1,122 transcripts (including non-coding SUTs, Table S1) showed statistically
149 significant differences in gene expression dynamics as a function of time between the two
150 strains (FDR cut-off 10%, when controlling for expression at t = 0h). While *TAO3* was

151 amongst the transcripts showing differential expression dynamics during sporulation (P =
152 0.004), none of its mitotic interactors showed differential expression (Figure 2B). However a
153 few *ACE2*-regulated genes did show differential expression (11 genes labeled green in Figure
154 2B), so we studied the effect of *ace2*Δ in the T strain and high sporulating SK1 strain. *ACE2*
155 is known to regulate the budding phenotype (Voth *et al.* 2005) thus both the T and SK1
156 strains with *ace2*Δ showed clumping. However *ace2*Δ did not affect sporulation efficiency of
157 either the T or SK1 strain (Figure 2C). Ace2-independent effect of RAM network on cellular
158 polarization have been observed previously (Nelson *et al*. 2003) therefore it is possible that
159 this network could still be involved in meiosis.
160
161 To determine whether the mitotic interactors of *TAO3* were distinct from its meiotic
162 interactors, we again used P_{Tet}-*TAO3(4477C)* strain and reduced *TAO3* expression only
163 during the mitotic growth phase, i.e. in glucose rich (YPD) medium. We observed no growth
164 difference between P_{Tet}-*TAO3(4477C)* strain with or without doxycycline and the T strain
165 (Figure S2). In addition there was no effect on sporulation efficiency among the strains
166 (Figure 1F). These results implied that probably *TAO3(4477C)* allele had a distinct meiotic
167 role from its established function in mitosis-related processes.
168
169 **Temporal gene expression profiling predicts *TAO3(4477C)*-specific interactors during**
170 **sporulation**
171 We showed that *TAO3(4477C)* had a distinct role in the sporulation processes within first 6h
172 of sporulation (Figure 1F). Hence we identified by clustering (see Methods), sets of
173 differentially expressed genes showing early and increasing trend in their expression profiles
174 in the T strain only. Various sporulation genes including crucial regulators of meiosis,
175 namely *IME1*, *IME2*, *DMC1* and *NDT80* were enriched ($P = 5.5 \times 10^{-12}$) in a cluster showing
176 increasing expression (Cluster II) during sporulation in the T strain (Figure 3B, see Methods).
177 Approximately 50% of Cluster II genes of the T strain showed a similar increasing trend in
178 the S strain, including *IME1*, *IME2*, *DMC1*, *ECM11* and *NDT80* (Figure S4, Table S2).
179 Interestingly very few early expressing genes (Cluster I) of the T strain overlapped with the S
180 (7%, Figure S4). These genes belonged to biological processes that regulated entry into
181 sporulation, such as carbohydrate metabolic process, ion transport, mitochondrial
182 organization and cellular respiration (Table 1). Furthermore genes involved in biological
183 processes like carbohydrate metabolic process and mitochondrial organization showed
184 repression in the S strain (Table 1, Figure S5). Therefore to study the early effects of the

185 causal *TAO3* allele, we identified regulators of only those differentially expressed genes that
186 showed early and increasing expression uniquely in the T strain (Tables S3 and S4).
187
188 These regulators were enriched in nutrient metabolism and chromatin modification –
189 biological processes important for initiation of meiosis (Neiman 2011). A core sporulation
190 gene *UME6*, which together with *IME1* induces expression of early meiotic genes (Kassir *et*
191 *al.* 2003) and is known to regulate other important processes for initiating meiosis (Table 2,
192 Lardenois *et al.* 2015) was also identified. Interestingly among the regulators of the genes
193 showing early and increasing expression uniquely in the T strain, we identified 25 upstream
194 regulators of *UME6* (Figure 4A, Tables S3-5). Among these regulators were *ERT1*, *OAF1-*
195 *PIP2* and *DAL81*. *ERT1*, a regulator of carbon source utilization (Turcotte *et al.* 2010) is
196 involved in the switch from fermentation to respiration in glucose-limiting conditions (Gasmi
197 *et al.* 2014). *OAF1-PIP2* is a protein complex regulating lipid metabolism (Karpichev and
198 Small 1998). *DAL81* is a regulator of nitrogen degradation pathway (Marzluf 1997).
199 Interestingly like *UME6*, *OAF1* target genes were repressed in the S strain (Cluster IV, Table
200 S6). Earlier work in S288c and SK1 strains has shown upregulation of *ERT1*, *PIP2* and
201 *DAL81* in SK1 strain during sporulation (Primig *et al.* 2000). However their deletion in
202 S288c strain had no effect on its sporulation efficiency (Deutschbauer *et al.* 2002). A few
203 other interesting candidate genes that were not upstream *UME6* were also identified (Tables
204 S3 and S4). These included *GAT1*, a regulator of nitrogen metabolism (Ljungdahl and
205 Daignan-Fornier 2012) and *GAT3*, a regulator of spore wall assembly (Lin *et al.* 2013). We
206 next tested if the metabolic regulators identified through this analysis were *TAO3(4477C)-*
207 specific mediating genes during sporulation.
208
209 **Allele-specific functional validation identifies *TAO3(4477C)*-specific genetic interactors**
210 **during sporulation**
211 The candidate genes predicted in the above analysis could be either causal mediating genes
212 interacting with *TAO3(4477C)* during sporulation or non-mediating consequential genes
213 associated with only the genotype or the phenotype. To identify only the causal mediating
214 genes, we used a genetic model described previously (Figure 4B, Gupta *et al.* 2015).
215 According to this model if a gene is associated only with the genotype and not with the
216 phenotype or is expressed as a consequence of the phenotype, its deletion would not affect
217 the T strain phenotype. If a gene had an independent role in sporulation phenotype, its
218 deletion will result in both a reduction in phenotype and an additive effect, irrespective of the

219 genetic background. Any significant deviation from this expectation would imply dependence
220 on the genotype with epistasis being an extreme case. In this scenario deleting the gene in T
221 strain would affect the phenotype while deleting the same in the S would not have an effect
222 on the phenotype, making it a causal mediating gene. While *gat1*Δ had no effect on
223 sporulation efficiency of the T strain, *ert1*Δ, *pip2*Δ and *gat3*Δ significantly reduced the mean
224 sporulation efficiency in the T strain by about 1.5-fold ($P = 2.1 \times 10^{-12}$, $P = 6.1 \times 10^{-13}$, $P =$
225 9.6×10^{-10} respectively, pair test in Methods, Figure 4C). Significant interaction terms were
226 obtained between the genetic backgrounds (S and T) and *ert1*Δ and *pip2*Δ ($P = 2.3 \times 10^{-4}$, $P =$
227 0.04, see Methods) but not for *gat3*Δ. This showed that the effect of *ert1*Δ and *pip2*Δ on
228 sporulation efficiency was specific to *TAO3(4477C)*, making them causal mediating genes.
229 *GAT1* and *GAT3* were non-mediating genes, the former associated with the genotype only or
230 a sporulation-consequential gene and the latter affected sporulation independent of the
231 genotype. Therefore genetic and functional validation using this model identified true causal
232 genes, namely *ERT1* and *PIP2*, mediating the effect of the allelic variant of *TAO3* on
233 sporulation efficiency.
234

235 **DISCUSSION**

236 Strong effects on phenotypic variation have been observed as a consequence of rare coding
237 variants (Cohen *et al*. 2004; Cohen *et al.* 2005). Tao3 is conserved from yeast to humans
238 (Hergovich *et al.* 2006) and had been functionally annotated solely for mitotic cell division
239 (Du and Novick 2002; Nelson *et al*. 2003) until it was mapped for sporulation efficiency
240 variation (Deutschbauer and Davis 2005). In this study we identify *ERT1* and *PIP2* as the
241 *TAO3(4477C)*-dependent mediators contributing to efficient meiosis. These genetic
242 interactors of *TAO3(4477C)* are distinct from the mitotic interactors of *TAO3(4477G)*. In this
243 study we identify their novel regulatory role in sporulation efficiency.
244

245 Acetate is the sole non-fermentable carbon source available to yeast during sporulation in
246 laboratory conditions. During sporulation, this acetate gets internalized into the tricarboxylic
247 acid (TCA) and glyoxylate cycle. Gluconeogenesis utilizes the TCA cycle intermediates and
248 synthesizes storage carbohydrates like trehalose that is utilized during late sporulation
249 processes (Ray and Ye 2013). Hence TCA, glyoxylate and gluconeogenic metabolic
250 processes are crucial for sporulation to proceed since reduced flux through these pathways
251 decreases sporulation efficiency (Aon *et al.* 1996). Moreover the genes encoding the crucial

252 enzymes of these metabolic processes such as *PFK1*, *CIT1* and *CIT2* are essential for
253 sporulation (Deutschbauer *et al.* 2002). *ERT1* and *PIP2* are known to regulate these
254 metabolic enzymes (Baumgartner *et al.* 1999; Gasmi *et al.* 2014). Taken all together, our
255 results suggest that the rare sporulation-associated *TAO3(4477C)* allele by interacting with
256 regulators of TCA cycle and gluconeogenic enzymes, modulates the metabolic flux early
257 during sporulation to result in a better sporulation efficiency.
258
259 *IME1* acts as a bottleneck for sporulation decision pathway. Lorenz and Cohen (2014)
260 observed that many sporulation-associated natural polymorphisms have been identified in
261 genes upstream or interacting with this input/output gene *IME1*. One of such polymorphic
262 genes *RIM15* is a nutrient-sensing regulator of *IME2*. While *TAO3* and *MKT1* (Gupta *et al.*
263 2015) do not directly regulate *IME1*, we show that variants in these two genes regulate early
264 upstream metabolic processes that impinge on *IME1*. Thus our study provides support for the
265 hypothesis that genes surrounding the signal transduction bottlenecks are reservoirs for
266 accumulating causal genetic variants.
267
268 During mitosis Tao3 localizes to polarized bud sites (Nelson *et al*. 2003). Further
269 determination of co-localization of *TAO3(4477C)* with membrane-associated *ERT1* and beta-
270 oxidation regulators *OAF1-PIP2* will give interesting clues of its function during sporulation.
271 Similar to other scaffolding proteins like *Fry* (*Drosophila*) and *SAX-2* (*C. elegans*), Tao3 has
272 multiple conserved Armadillo-like repeats (Hergovich *et al.* 2006) and the causal sporulation
273 variant is present in one of them. Tao3(1493E) physically interacts with the RAM network
274 proteins in rich growth conditions. It would be interesting to determine binding partners of
275 Tao3(1493Q) during sporulation and if the variant affects the binding of this putative
276 scaffolding protein. Additionally a few genes enriched for iron metabolism were
277 differentially expressed during growth phase prior to incubation in the sporulation medium (t
278 = 0h). It would be interesting to study whether this metabolic effect of *TAO3* also plays a role
279 in sporulation.
280
281 Even if the basic cellular network of an organism is known, it is crucial to understand how
282 natural genetic variation and stress conditions modulate the molecular interactions within this
283 network resulting in differences in phenotypic outcomes (Gasch *et al.* 2016). Studies, such as
284 this work, aimed at understanding the molecular consequences of genetic variation are
285 especially important in the field of personalized medicine to make more reliable predictions

286 regarding the functional consequences of an individual's genotype on disease predisposition
287 and treatment (Burga and Lehner 2013).
288

289 # MATERIALS AND METHODS

290 **Yeast strains and media**

291 The yeast strains were grown in standard conditions at 30˚C in YPD (1% Yeast extract, 2%
292 Bacto peptone, 2% dextrose). Allele replacement strain YAD331 (Deutschbauer and Davis
293 2005) was a S288c-background diploid strain containing the homozygous causative
294 sporulation polymorphism *TAO3(4477C)*. Whole-genome resequencing of YAD331 with
295 S288c strain as the reference strain identified two additional polymorphisms (Figure S6,
296 Table S7). Three consecutive backcrosses were performed between the haploid derivative of
297 YAD331 and the haploid reference strain (S288c) to remove these secondary polymorphisms.
298 After the backcrosses, the sole genetic difference between the reference S288c strain and the
299 backcrossed allele replacement strain was at *TAO3(G4477C)* position, which was confirmed
300 by performing PCR-based sequencing 650bp up and downstream around the two secondary
301 polymorphisms and the *TAO3* polymorphic nucleotide. This backcrossed strain was
302 diplodized to make it homozygous at *TAO3(4477C)* position and was termed as "T strain" in
303 this study. The diploid parental strain S288c was termed as "S strain" in the study. All gene
304 deletions in the study were made in the haploids of T and S strains except the ones made in
305 SK1 strain (Table S8). Deletions were performed and verified as described previously
306 (Goldstein and McCusker 1999; Gietz and Woods 2002). The haploid strains were diplodized
307 using pHS2 plasmid (containing a functional *HO*) and mating type were confirmed by
308 performing MAT PCR (Huxley *et al.* 1990). All the experiments in this study were
309 performed using the diplodized parent strains and their diploid derivatives. For replacing the
310 endogenous *TAO3* promoter (-150 to -1bp upstream start site) in the T strain with a
311 tetracycline-responsive promoter, a $tetO_7$-based promoter substitution cassette containing
312 *kanMX4* was amplified from the plasmid pCM225 (Bellí *et al*. 1998b). The diploid T strain
313 with this $tetO_7$-based cassette is termed P_{Tet}-*TAO3(4477C)* strain. The primers for
314 sequencing, deletions and their confirmations are listed in Table S9.
315

316 **Phenotyping**

317 Sporulation efficiency estimation at 48h, progression through meiotic landmark events
318 Meiosis I (MI) and Meiosis II (MII) and its quantitation was done as described previously

319 (Gupta *et al.* 2015). For quantitation of meiotic landmarks in the T strain, parametric curves
320 assuming delayed and 1st order kinetics were fitted to the DAPI-stained meiotic progression
321 time course data and fitting uncertainties were estimated by bootstrapping (File S1). Cell
322 cycle progression data for S288c and SK1 strains was taken from Gupta *et al.* (2015) (Figure
323 1D-E). Conditional expression of *TAO3(4477C)* was performed by constructing P_{Tet}-*TAO3*
324 strain (details in File S1), which was responsive to tetracycline-analogue doxycycline (Bellí
325 *et al*. 1998a; Bellí *et al.* 1998b). Doxycycline (2µg/ml) was added in growth and sporulation
326 media to decrease the expression of *TAO3* gene. For each strain, a minimum of three
327 biological replicates was used and the experiment was carried out a minimum of two times.
328 Approximately 300 cells were counted per replicate. Fold difference was calculated as the
329 ratio of mean sporulation efficiencies of the two strains A and B when the sporulation
330 efficiency of A is greater than of B. Growth curve analysis was performed for individual
331 strains grown in YPD in 96-well plates. Cells were grown overnight in YPD to saturation, re-
332 inoculated in YPD in transparent 96-well plates with a starting OD_{600} of 0.01 and grown with
333 shaking at 30˚C for 24h in Tecan Infinite M200 microplate reader. Doubling times were
334 calculated from OD measurements of liquid cultures at a wavelength of 600 nm in the Tecan
335 reader. For each strain, four technical replicates for each of the three biological replicates
336 were used. Raw sporulation efficiency values are given in Table S10.
337
338 **Statistical test for calculating sporulation efficiency**
339 For comparing sporulation efficiency, two statistical tests were used: the pair test and the
340 interaction test. The pair test tests the null hypothesis that the two given strains (S and T)
341 have the same sporulation efficiency.
342
343 The number $y_{i,k}$ of sporulated cells (4-nuclei count) among the total number of cells $n_{i,k}$ of
344 strain *i* in replicate experiment *k* was modeled with a quasi-binomial generalized linear model
345 using the *logit* link function and subject to a common log-odd ratio β_i between replicates, i.e.:
346
347 $$\log\left(\frac{\mu_{i,k}}{n_{i,k}-\mu_{i,k}}\right)=\beta_i \text{ for all } k,$$
348 where $\mu_{i,k}=E\left(y_{i,k}\right)$.
349

350 The pair test tests the null hypothesis of equality of log odd-ratios for two strains *i* and *j*, i.e.
351 $H_0 : \beta_i = \beta_j$.
352
353 In the case of the S and T strains, the interaction test tests the null hypothesis that the effect
354 of mutation A is independent of the effect of mutation B taking the T strain as reference
355 background. This test thus compares four strains: mutation A only, mutation B only, both A
356 and B and neither A nor B (T strain). Here the S strain was considered as a T strain mutated
357 for *TAO3(4477)*. For every interaction test, we considered the dataset of the four strains of
358 interest and fitted a quasi-binomial generalized linear model using the *logit* link function and
359 subject to:
360

361 $$\log\left(\frac{\mu_{i,k}}{n_{i,k} - \mu_{i,k}}\right) = \beta_0 + \beta_A A_i + \beta_B B_i + \beta_{A,B} A_i B_i \text{ for all } k,$$

362 where A_i and B_i are indicator variables of the mutations A and B in strain *i* respectively. The
363 interaction test tested the null hypothesis that the odd ratio of sporulation in the double
364 mutant equals the product of the odd ratios of each mutation, i.e. $H_0 : \beta_{A,B} = 0$.
365
366 Both the pair test and the interaction test were implemented in the statistical language R with
367 the function *glm()* assuming a constant variance function fitted by maximizing the quasi-
368 likelihood and using the t-test on the tested parameters (Gupta *et al.* 2015).
369
370 **Whole genome gene-expression profiling**
371 Sporulating yeast cell collection at 0h, 30m, 45m, 1h10m, 1h40m, 2h30m, 3h50m, 5h40m
372 and 8h30m (logarithmic time-series), RNA isolation and cDNA preparation were performed
373 as previously described (Xu *et al.* 2009). Samples were hybridized to *S. cerevisiae* yeast
374 tiling array (Affymetrix, Cat# 520055). Arrays at each time point for both the strains were
375 normalized together using *vsn* normalization method (Huber *et al.* 2002). For qPCR, aliquots
376 of cDNA were used in real-time PCR analyses with reagents from Kapa SYBR fast Universal
377 qPCR master mix (Kapa Biosystems) in the Eppendorf Real-time PCR system according to
378 manufacturer's protocol. For each strain, four technical replicates for each of the three
379 biological replicates were used. The primers used are given in Table S9.
380

381 **Whole genome gene-expression analysis**

382 Within each strain, the $\log_2$ expression values obtained were smoothed using *locfit* at
383 optimized bandwidth parameter $h = 1.2$ (Figure S7), base transformed for each transcript by
384 subtracting the expression value at each time point from the baseline value at time point t =
385 0h (t_0, Table S11). This $\log_2$ fold change value with respect to t_0 is described as "expression"
386 throughout the manuscript. For identifying the genes showing temporal differential
387 expression between the T and S strains (Table S1), method implemented in EDGE software
388 was used, which calculated statistically significant changes in expression between the T and
389 S strains over time (Storey *et al.* 2005). The differentially expressed genes were clustered
390 according to their temporal expression patterns using time abstraction clustering algorithm
391 implemented in the TimeClust software (Magni *et al.* 2008, see File S1). Four major clusters
392 were identified in each strain: Cluster I (early trend), Cluster II (increasing trend), Cluster III
393 (late trend), Cluster IV (repressing trend) (Table S2). The transcription factors regulating a
394 cluster of genes were extracted using the YEASTRACT database (Teixeira *et al.* 2013). Only
395 those transcription factors were considered as candidate genes whose target genes were
396 significantly enriched in the corresponding cluster ($P \leq 0.05$, odds ratio ≥ 1.5). YEASTRACT
397 database was also used to obtain the regulation matrix of yeast for identifying target genes of
398 regulators in this study such as *UME6*. Target genes for *ACE2* were obtained from Nelson *et*
399 *al.* (2003). Significantly enriched Gene Ontology terms by biological process (Bonferroni
400 corrected $P < 0.05$, Table 1) were obtained from SGD Yeastmine (Balakrishnan *et al.* 2012).

401

402 **Data availability**

403 The array data for the T strain has been deposited in ArrayExpress
404 (http://www.ebi.ac.uk/arrayexpress/) with accession number E-MTAB-3889. The whole
405 genome sequence data for the T strain has been deposited in the European Nucleotide
406 Archive (http://www.ebi.ac.uk/ena/) with the accession number PRJEB8698. The rest of the
407 data are available as Supporting Information. The array data and the whole genome sequence
408 data for the S strain were downloaded from Gupta *et al.* (2015). *TAO3* gene sequence data for
409 SGRP strains (Liti *et al.* 2009) was downloaded from
410 (http://www.moseslab.csb.utoronto.ca/sgrp/). Additional 24 *TAO3* sequences were
411 downloaded from Saccharomyces Genome Database (SGD,
412 http://www.yeastgenome.org/cgi-bin/FUNGI/alignment.pl?locus=YIL129C, date accessed:
413 01 March 2016).

414

415 ## ACKNOWLEDGEMENTS

416 We thank Manu Tekkedil for help with whole genome sequencing sample preparation and
417 Allan Jones and Gyan Bhanot for helpful comments. This research was supported by Tata
418 Institute of Fundamental Research intramural funds and Department of Biotechnology grant
419 BT/PR14842/BRB/10/881/2010 (H.S.); Bavarian Research Center for Molecular Biosystems
420 and Bundesministerium für Bildung und Forschung through the Juniorverbund in der
421 Systemmedizin "mitOmics" grant FKZ 01ZX1405A (J.G.); the National Institutes of Health,
422 Deutsche Forschungsgemeinschaft and a European Research Council Advanced Investigator
423 Grant (L.M.S.). The funders had no role in study design, data collection and analysis,
424 decision to publish, or preparation of the manuscript.

425

426 # TABLES

427 **Table 1. Functional GO categories of clusters in the T and S strains**

Cluster	Functional GO category	Genes
Early in T strain (Cluster I)	Carbohydrate metabolic process	*DOG1*, *YPI1*
	Ion transport	*AVT4*, *DAL5*
	Mitochondrion organization	*PPE1*, *UPS3*
	Cellular respiration	*COX5B*
Early in T strain (Cluster I) repressed in S strain (Cluster IV)	Carbohydrate metabolic process	*ALG6*, *DEP1*, *DOG1*, *TPS3*, *YPI1*
	Mitochondrial organization	*ATG33*, *COX20*, *PPE1*, *UPS3*

428

429 Comparison of functional GO categories of differentially expressed genes in the T strain
430 clusters with the S strain. See Table S2 for the full list of genes in each cluster.

431

432 **Table 2. Functional GO categories of regulators of clusters in the T and S strains**

Functional GO category	Regulators	*P* value
Carbon metabolism	*ERT1*, *OAF1*, *PIP2*, *MIG1*, *MIG2*	1.9×10^{-6}
Nitrogen catabolite regulation	*DAL81*, *DAL82*, *GAT1*, *UME6*	1.7×10^{-5}
Chromatin modification	*ISW1*, *PHO2*, *PHO4*, *UME6*, *OAF1*, *XBP1*, *SIF2*, *RSC2*	1.4×10^{-5}

433

434 Functional GO classification of the regulators of the differentially expressed genes showing
435 early and increasing expression only in the T strain. See Tables S3 and S4 for the full list of
436 genes.

437

438 # FIGURE LEGENDS

439 **Figure 1. Role of *TAO3* in sporulation efficiency**

440 (A) Comparison of genomic sequence of *TAO3* (4,441-4,500) across the SGRP collection
441 (Liti *et al.* 2009). The 4,477th position of *TAO3* consists of the sporulation causative variant
442 where identical nucleotides are indicated by the same color. Identity indicates the percentage
443 match between the nucleotides in the shown region of the gene. The strains are ordered
444 according to their mean sporulation efficiency (Tomar *et al.* 2013): high (60-100%),
445 intermediate (10-60%), low (0-10%) and ND (not determined).

446 (B) Bar plots represents the mean sporulation efficiency after 48h of the SK1, T and S strains.
447 The sporulation efficiency data is indicated as circles.

448 (C) Line graphs represent the mean sporulation efficiency of the S, T and SK1 strains
449 measured till saturation, i.e. till sporulation efficiency did not vary for 3 consecutive days.

450 (D) Percentage of 1-, 2- and 4-nuclei states of the T strain (y-axis) versus time in sporulation
451 medium (x-axis). 1-nucleus stage is indicated as red circles (G_0/G_1 phase), 2-nuclei state as
452 yellow circles (completion of Meiosis I, MI phase) and blue circles is 4-nuclei stage
453 (completion of Meiosis II, MII phase).

454 (E) Bootstrap distribution of the time to initiate meiosis and the rate of transition from G_1/G_0
455 into MI, estimated from time courses in (D). See Methods for details.

456 (F) Conditional expression of *TAO3(4477C)* during sporulation in P_{Tet}-*TAO3(4477C)* strain
457 (indicated as P_{Tet}). Y-axis is the mean sporulation efficiency in 48h. No doxycycline in
458 growth (YPD) or spo (YPA + sporulation) medium is depicted as "-" condition on x-axis and
459 addition of doxycycline is depicted as "+" in that condition. "+3h" condition in Spo implies
460 doxycycline was throughout in the growth medium and in the sporulation medium till 3h
461 after which cells were sporulated in the absence of doxycycline. "+6h" condition implies
462 doxycycline was throughout in the growth medium and in the sporulation medium till 6h
463 after which cells were sporulated in the absence of doxycycline. *P* value was calculated by an
464 unpaired t-test. Error bars are standard error of mean.

465 **Figure 2. Role of *TAO3* in meiosis is distinct from its role during mitosis**

466 (A) Heatmap showing gene expression of RAM network genes and Ace2-regulated genes in
467 the T and S strains. Gene names in green show differential expression (data in Tables S1 and
468 S11).

469 (B) Bar plots represent the mean sporulation efficiency after 48h of the SK1 and T wild type
470 (wt) and *ace2*Δ deletion strains. Pair and interaction tests (described in Methods) were
471 performed to test significance.
472 (C) Expression profile ($\log_2$ fold change t_0) of *TAO3* is given in the y-axis for the T (purple)
473 and S strains (red) and the x-axis denotes the time in sporulation medium (data in Tables S1
474 and S11).
475
476 **Figure 3. Global gene expression variation in presence of causative *TAO3* allele**
477 (A) Temporal heat map of meiotic genes in the T and S strains. The gene names shown in
478 green are differentially expressed in the presence of *TAO3(4477C)*.
479 (B) The expression profile ($\log_2$ fold change t_0) for the meiotic landmark genes is given in the
480 y-axis and the x-axis denotes the time in sporulation medium. Red line represents the
481 expression profile of the respective gene in the S strain and blue line is the same in the T
482 strain.
483 (C) Heat map of the T and S strains showing differentially expressed gene across time within
484 each cluster. Each row represents a single gene and columns are time points of each strain
485 (for gene list in each cluster see Table S2). The order of genes in the two strains is based on
486 the clustering of the T strain. Functional GO categories of genes in each cluster are shown on
487 left. The boxplots shown on right represent the average expression profile of each cluster in
488 the T and S strains. The number of genes in each cluster in a strain is indicated in brackets.
489
490 **Figure 4. Identifying candidate genes mediating the allele specific effects of *TAO3***
491 **during sporulation using the temporal gene expression data**
492 (A) Regulatory network of candidate genes predicted to mediate the effects of *TAO3(4477C)*
493 in sporulation. The candidate mediating genes are shown as bigger nodes (large circles) with
494 their target genes (small circles) connected to them as straight lines. The box contains the
495 protein network interactions of the candidate genes with the core sporulation gene *UME6*,
496 obtained from YEASTRACT (see Methods). Colors inside the nodes were calculated as an
497 average of the first six time points in sporulation (early phase). For complete list of
498 interacting genes and their expression values, see Tables S5 and S11, respectively.
499 (B) Genetic model for functional validation of allele-specific interactors mediating
500 sporulation efficiency variation. Wild type effect comparison of the two alleles A1 and A2 of
501 *YFG1* gene is shown inside the box. A1 is associated with high sporulation efficiency (wild
502 type genotype and phenotype shown) and A2 is associated with low sporulation efficiency

503 (wild type genotype and phenotype shown). Genetic interaction of these *YFG1* alleles with
504 candidate mediating genes (*YFG2*) is represented – (i) Representation of non-mediating gene
505 associated with genotype only or is a consequence of the phenotype since *yfg2*Δ in the
506 presence of A1 does not affect the wild type phenotype of A1; (ii) Representation of non-
507 mediating gene associated with the phenotype independent of the allele since *yfg2*Δ in the
508 presence of both A1 and A2 lowers (low) the phenotype; (iii) Representation of causal
509 mediating gene since *yfg2*Δ only in presence of allele A1 lowers the phenotype and in the
510 presence of allele A2 does not change the wild type phenotype of A2.
511 (C) Bar plots represent the mean sporulation efficiency after 48h of the T and S wild type
512 (wt) and *ert1*Δ, *pip2*Δ and *gat3*Δ strains. Pair and interaction tests (see Methods) were
513 performed to test significance.
514

515 # SUPPORTING INFORMATION

516 **File S1.** Detailed methods
517 **Table S1.** Differentially expressed genes between the T and S strains with their *P* and *Q*
518 values calculated using EDGE
519 **Table S2.** Genes in each cluster using TimeClust
520 **Table S3.** Transcription factors regulating unique early (Cluster I) genes of the T strain
521 **Table S4.** Transcription factors regulating unique increasing (Cluster II) genes of the T strain
522 **Table S5.** Differentially expressed target genes of regulators of candidate genes mediating
523 the affect of *TAO3*
524 **Table S6.** Transcription factors regulating unique repressing (Cluster IV) genes of the S
525 strain
526 **Table S7.** Whole genome resequencing results for the *TAO3* allele replacement strain
527 **Table S8.** Strain list
528 **Table S9.** Primer list
529 **Table S10.** Raw sporulation efficiency values
530 **Table S11.** Smoothed expression data, base transformed with respect to t_0 for the T and S
531 strains
532 **Figure S1.** Mathematical modeling to identify stages of meiosis affected by *TAO3* causal
533 allele
534 **Figure S2.** Growth phenotype and *TAO3* expression in P_{Tet}-*TAO3(4477C)* strain
535 **Figure S3.** Comparison of global gene expression between the T and S strains at t = 0h

536 **Figure S4.** Comparison of genes showing early (Cluster I) and increasing trend (Cluster II)
537 between the T and S strains
538 **Figure S5.** Genes having early expression in the T strain show expression at later time points
539 or repressed in the S strain
540 **Figure S6.** Whole genome resequencing of *TAO3* allele replacement strain (YAD331,
541 (Deutschbauer and Davis 2005) in comparison to the S288c reference strain
542 **Figure S7.** Smoothing of normalized temporal data using *locfit*
543

544 # REFERENCES

545 Aon, J. C., V. A. Rapisarda, and S. Cortassa, 1996 Metabolic fluxes regulate the success of
546 sporulation in *Saccharomyces cerevisiae*. Exp Cell Res 222: 157–162.
547 Balakrishnan, R., J. Park, K. Karra, B. C. Hitz, G. Binkley *et al.*, 2012 YeastMine – an
548 integrated data warehouse for *Saccharomyces cerevisiae* data as a multipurpose tool-kit.
549 Database (Oxford) 2012: bar062–bar062.
550 Baumgartner, U., B. Hamilton, M. Piskacek, H. Ruis, and H. Rottensteiner, 1999 Functional
551 analysis of the Zn_2Cys_6 transcription factors Oaf1p and Pip2p – different roles in fatty
552 acid induction of β-oxidation in *Saccharomyces cerevisiae*. J Biol Chem 274: 22208–
553 22216.
554 Bellí, G., E. Garí, M. Aldea, and E. Herrero, 1998a Functional analysis of yeast essential
555 genes using a promoter-substitution cassette and the tetracycline-regulatable dual
556 expression system. Yeast 14: 1127–1138.
557 Bellí, G., E. Garí, L. Piedrafita, M. Aldea, and E. Herrero, 1998b An activator/repressor dual
558 system allows tight tetracycline-regulated gene expression in budding yeast. Nucleic
559 Acids Res 26: 942–947.
560 Bogomolnaya, L. M., R. Pathak, J. Guo, and M. Polymenis, 2006 Roles of the RAM
561 signaling network in cell cycle progression in *Saccharomyces cerevisiae*. Curr Genet 49:
562 384–392.
563 Burga, A., and B. Lehner, 2013 Predicting phenotypic variation from genotypes, phenotypes
564 and a combination of the two. Curr Opin Biotechnol 24: 803–809
565 Cirulli, E. T., and D. B. Goldstein, 2010 Uncovering the roles of rare variants in common
566 disease through whole-genome sequencing. Nat Rev Genet 11: 415–425.
567 Cohen, J., A. Pertsemlidis, I. K. Kotowski, R. Graham, C. K. Garcia *et al.*, 2005 Low LDL
568 cholesterol in individuals of African descent resulting from frequent nonsense mutations
569 in *PCSK9*. Nat Genet 37: 161–165.
570 Cohen, J. C., R. S. Kiss, A. Pertsemlidis, Y. L. Marcel, R. McPherson *et al*., 2004 Multiple
571 rare alleles contribute to low plasma levels of HDL cholesterol. Science 305: 869–872.
572 Deutschbauer, A. M., and R. W. Davis, 2005 Quantitative trait loci mapped to single-
573 nucleotide resolution in yeast. Nat Genet 37: 1333–1340.
574 Deutschbauer, A. M., R. M. Williams, A. M. Chu, and R. W. Davis, 2002 Parallel phenotypic
575 analysis of sporulation and postgermination growth in *Saccharomyces cerevisiae*. Proc
576 Natl Acad Sci U S A 99: 15530–15535.
577 Du, L. L., and P. Novick, 2002 Pag1p, a novel protein associated with protein kinase Cbk1p,
578 is required for cell morphogenesis and proliferation in *Saccharomyces cerevisiae*. Mol
579 Biol Cell 13: 503–514.
580 Gagneur, J., O. Stegle, C. Zhu, P. Jakob, M. M. Tekkedil *et al.*, 2013 Genotype-environment

581 interactions reveal causal pathways that mediate genetic effects on phenotype. PLoS
582 Genet 9: e1003803.
583 Gasch, A. P., B. A. Payseur, and J. E. Pool, 2016 The power of natural variation for model
584 organism biology. Trends Genet 32: 147–154.
585 Gasmi, N., P. E. Jacques, N. Klimova, X. Guo, A. Ricciardi *et al.*, 2014 The switch from
586 fermentation to respiration in *Saccharomyces cerevisiae* is regulated by the Ert1
587 transcriptional activator/repressor. Genetics 198: 547–560.
588 Gerke, J., K. Lorenz, and B. Cohen, 2009 Genetic interactions between transcription factors
589 cause natural variation in yeast. Science 323: 498–501.
590 Gietz, D. R., and R. A. Woods, 2002 Transformation of yeast by lithium acetate/single-
591 stranded carrier DNA/polyethylene glycol method. Methods Enzymol 350: 87–96.
592 Goldstein, A. L., and J. H. McCusker, 1999 Three new dominant drug resistance cassettes for
593 gene disruption in *Saccharomyces cerevisiae*. Yeast 15: 1541–1553.
594 Granek, J. A., Ö. Kayıkçı, and P. M. Magwene, 2011 Pleiotropic signaling pathways
595 orchestrate yeast development. Curr Opin Microbiol 14: 676–681.
596 Gupta, S., A. Radhakrishnan, P. Raharja-Liu, G. Lin, L. M. Steinmetz *et al.*, 2015 Temporal
597 expression profiling identifies pathways mediating effect of causal variant on phenotype.
598 PLoS Genetics 11: e1005195.
599 Gurvitz, A., F. Suomi, H. Rottensteiner, J. K. Hiltunen, and I. W. Dawes, 2009 Avoiding
600 unscheduled transcription in shared promoters: *Saccharomyces cerevisiae* Sum1p
601 represses the divergent gene pair *SPS18-SPS19* through a midsporulation element (MSE).
602 FEMS Yeast Res 9: 821–831.
603 Hergovich, A., M. R. Stegert, D. Schmitz, and B. A. Hemmings, 2006 NDR kinases regulate
604 essential cell processes from yeast to humans. Nat Rev Mol Cell Biol 7: 253–264.
605 Huber, W., A. von Heydebreck, H. Sültmann, A. Poustka, and M. Vingron, 2002 Variance
606 stabilization applied to microarray data calibration and to the quantification of
607 differential expression. Bioinformatics 18: S96–S104.
608 Huxley, C., E. D. Green, and I. Dunham, 1990 Rapid assessment of *S. cerevisiae* mating type
609 by PCR. Trends Genet 6: 236.
610 Jambhekar, A., and A. Amon, 2008 Control of meiosis by respiration. Current Biol 18: 969–
611 975.
612 Karpichev, I. V., and G. M. Small, 1998 Global regulatory functions of Oaf1p and Pip2p
613 (Oaf2p), transcription factors that regulate genes encoding peroxisomal proteins in
614 *Saccharomyces cerevisiae*. Mol Cell Biol 18: 6560–6570.
615 Kassir, Y., N. Adir, E. Boger-Nadjar, N. G. Raviv, I. Rubin-Bejerano *et al.*, 2003
616 Transcriptional regulation of meiosis in budding yeast. Int Rev Cytol 224: 111–171.
617 Lardenois, A., E. Becker, T. Walther, M. J. Law, B. Xie *et al.*, 2015 Global alterations of the
618 transcriptional landscape during yeast growth and development in the absence of Ume6-
619 dependent chromatin modification. Mol Genet Genomics 290: 2031–2046.
620 Lee, J. H., M. Huynh, J. L. Silhavy, S. Kim, T. Dixon-Salazar *et al.*, 2012 *De novo* somatic
621 mutations in components of the PI3K-AKT3-mTOR pathway cause
622 hemimegalencephaly. Nat Genet 44: 941–945.
623 Lin, C. P., C. Kim, S. O. Smith, and A. M. Neiman, 2013 A highly redundant gene network
624 controls assembly of the outer spore wall in *S. cerevisiae*. PLoS Genetics 9: e1003700.
625 Liti, G., D. M. Carter, A. M. Moses, J. Warringer, L. Parts *et al.*, 2009 Population genomics
626 of domestic and wild yeasts. Nature 458: 337–341.
627 Ljungdahl, P. O., and B. Daignan-Fornier, 2012 Regulation of amino acid, nucleotide, and
628 phosphate metabolism in *Saccharomyces cerevisiae*. Genetics 190: 885–929.
629 Lorenz, K., and B. A. Cohen, 2014 Causal variation in yeast sporulation tends to reside in a
630 pathway bottleneck. PLoS Genet 10: e1004634.

631 Magni, P., F. Ferrazzi, L. Sacchi, and R. Bellazzi, 2008 TimeClust: a clustering tool for gene
632 expression time series. Bioinformatics 24: 430–432.
633 Manolio, T. A., F. S. Collins, N. J. Cox, D. B. Goldstein, L. A. Hindorff *et al.*, 2009 Finding
634 the missing heritability of complex diseases. Nature 461: 747–753.
635 Marzluf, G. A., 1997 Genetic regulation of nitrogen metabolism in the fungi. Microbiol Mol
636 Biol Rev 61: 17–32.
637 Neiman, A. M., 2005 Ascospore Formation in the yeast *Saccharomyces cerevisiae*. Microbiol
638 Mol Biol Rev 69: 565–584.
639 Neiman, A. M., 2011 Sporulation in the budding yeast *Saccharomyces cerevisiae*. Genetics
640 189: 737–765.
641 Nelson, B., C. Kurischko, J. Horecka, M. Mody, P. Nair, *et al*., 2003 RAM: A conserved
642 signaling network that regulates Ace2p transcriptional activity and polarized
643 morphogenesis. Mol Biol Cell 14: 3782–3803.
644 Primig, M., R. M. Williams, E. A. Winzeler, G. G. Tevzadze, A. R. Conway, *et al.*, 2000 The
645 core meiotic transcriptome in budding yeasts. Nat Genet 26: 415–423.
646 Ray, D., and P. Ye, 2013 Characterization of the metabolic requirements in yeast meiosis.
647 PLoS ONE 8: e63707.
648 Saint Pierre, A., and E. Génin, 2014 How important are rare variants in common disease?
649 Brief Funct Genomics 13: 353–361.
650 Spellman, P. T., G. Sherlock, M. Q. Zhang, V. R. Iyer, K. Anders *et al.*, 1998 Comprehensive
651 identification of cell cycle-regulated genes of the yeast *Saccharomyces cerevisiae* by
652 microarray hybridization. Mol Biol Cell 9: 3273–3297.
653 Stankiewicz, P., and J. R. Lupski, 2010 Structural variation in the human genome and its role
654 in disease. Annu Rev Med 61: 437–455.
655 Storey, J. D., W. Xiao, J. T. Leek, R. G. Tompkins, and R. W. Davis, 2005 Significance
656 analysis of time course microarray experiments. Proc Natl Acad Sci U S A 102: 12837–
657 12842.
658 Teixeira, M. C., P. T. Monteiro, J. F. Guerreiro, J. P. Gonçalves, N. P. Mira *et al.*, 2013 The
659 YEASTRACT database: an upgraded information system for the analysis of gene and
660 genomic transcription regulation in *Saccharomyces cerevisiae*. Nucleic Acids Res 42:
661 D161–D166.
662 Tomar, P., A. Bhatia, S. Ramdas, L. Diao, G. Bhanot *et al.*, 2013 Sporulation genes
663 associated with sporulation efficiency in natural isolates of yeast. PLoS ONE 8: e69765.
664 Turcotte, B., X. B. Liang, F. Robert, and N. Soontorngun, 2010 Transcriptional regulation of
665 nonfermentable carbon utilization in budding yeast. FEMS Yeast Res 10: 2–13.
666 Voth, W. P., A. E. Olsen, M. Sbia, K. H. Freedman, and D. J. Stillman, 2005 *ACE2*, *CBK1*,
667 and *BUD4* in budding and cell separation. Eukaryotic Cell 4: 1018–1028.
668 Xu, Z., W. Wei, J. Gagneur, F. Perocchi, S. Clauder-Münster *et al.*, 2009 Bidirectional
669 promoters generate pervasive transcription in yeast. Nature 457: 1033–1037.
670 Zuk, O., S. F. Schaffner, K. Samocha, R. Do, E. Hechter *et al.*, 2014 Searching for missing
671 heritability: designing rare variant association studies. Proc Natl Acad Sci U S A 111:
672 E455–E464.
673

Gupta_*et*_*al*_Figure 1

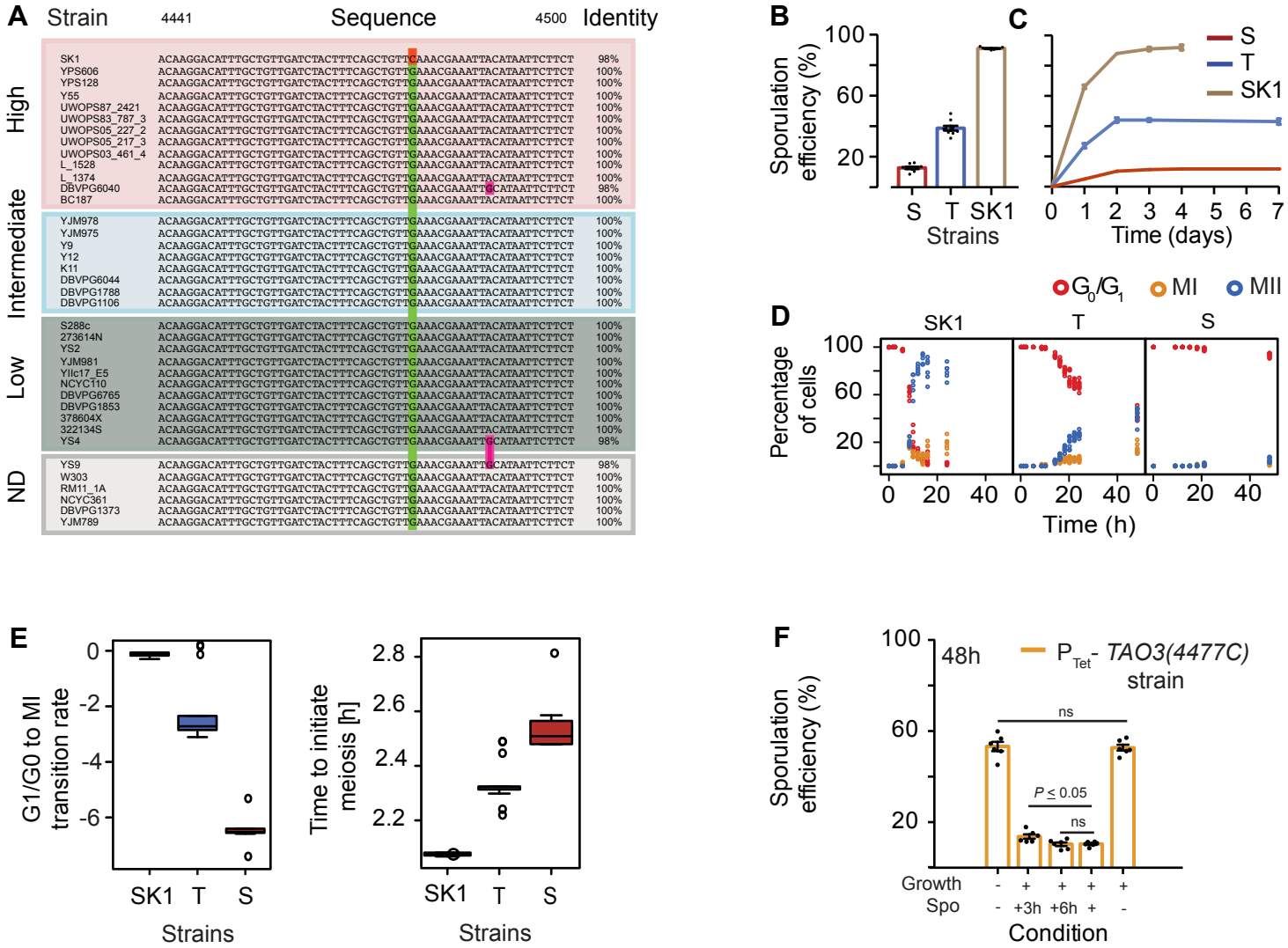

Gupta_*et*_*al*_Figure 2

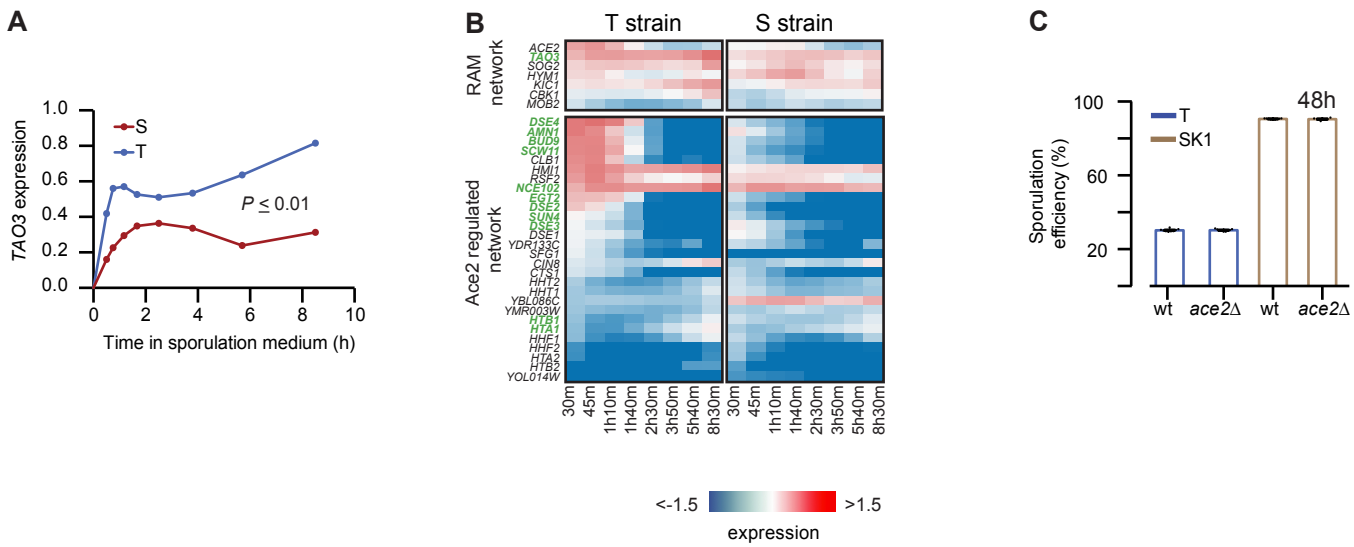

Gupta_*et al*_Figure 3

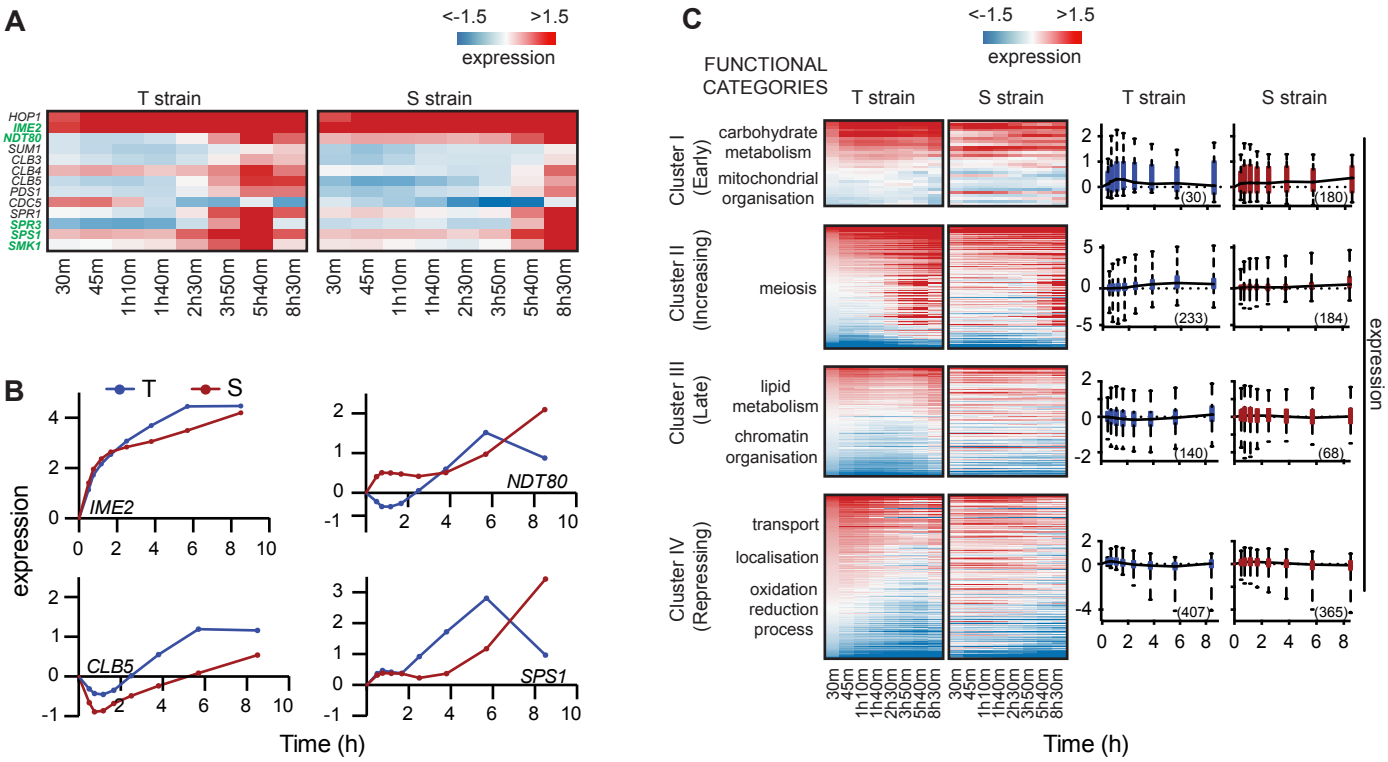
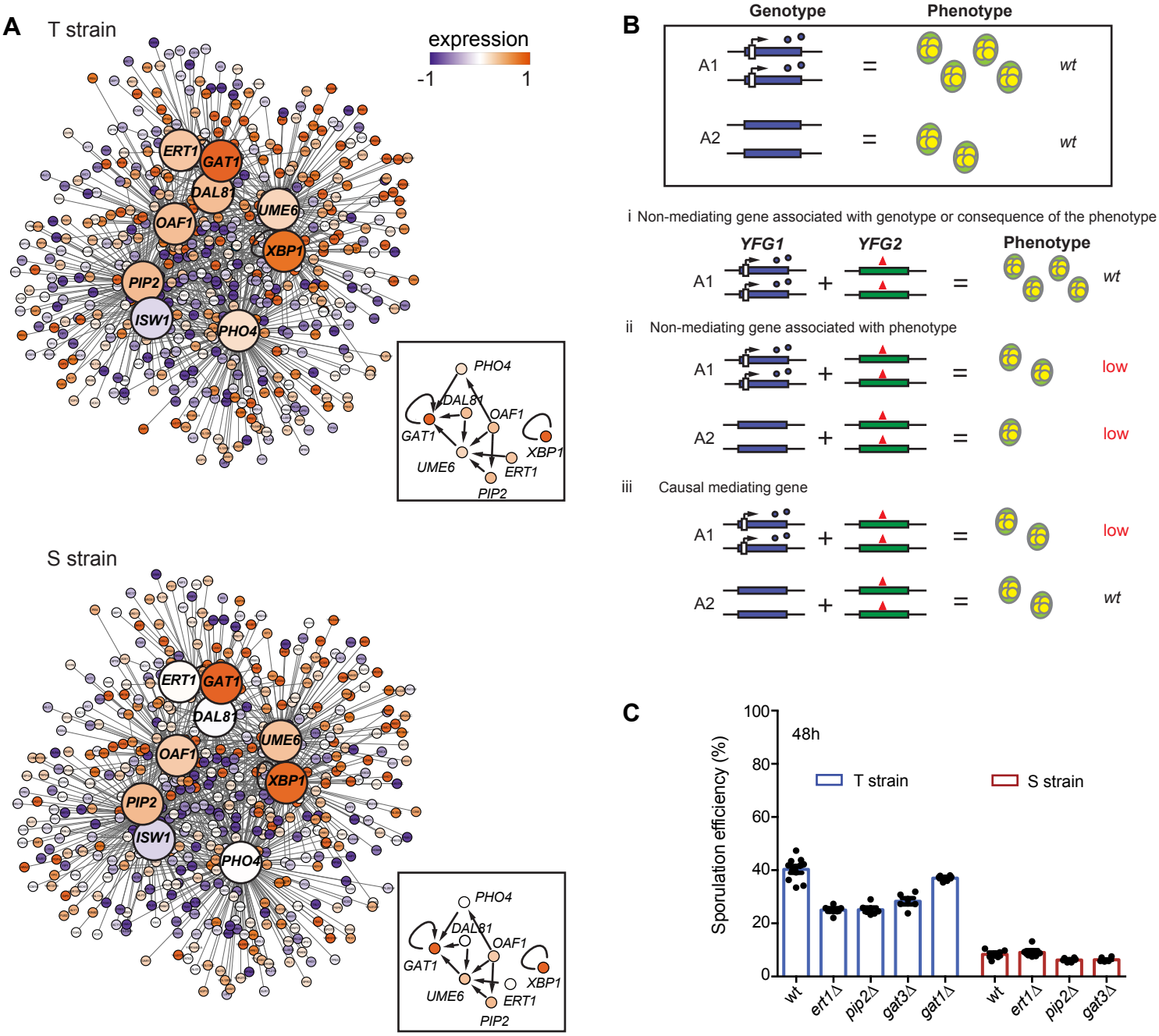
Gupta_*et al*_Figure 4